

# Generation of a Porous Luminescent Structure Through Ultrasonically Induced Pathways of Silicon Modification\*\*

Ekaterina V. Skorb,\* Daria V. Andreeva, and Helmuth Möhwald

In heterogeneous solid–liquid systems, cavitation can induce three main effects: 1) Surface damage can occur at the liquid–solid interface through both symmetric bubble collapse, resulting in shock waves and subsequent microstreaming,<sup>[1]</sup> and asymmetric bubble collapse, resulting in surface microjets that are several orders of magnitude larger than the cavitation bubble size. For example, at 20 kHz, the maximum size of a cavitation bubble is approximately 50  $\mu\text{m}$ .<sup>[2]</sup> 2) Chemical surface modification/stabilization owing to ultrasonic free-radical formation<sup>[1]</sup> can occur. 3) Fragmentation of brittle solids and an increase in their surface area can occur through high-velocity interparticle collisions in suspensions of solid species (Figure 1).<sup>[1,2]</sup>

Recently, we have demonstrated the effect of ultrasound on the phase transitions in metal particles.<sup>[3]</sup> The ultrasonication of metals has been found to cause crystal deformation, cleavage of chemical bonds, and phase transformations between amorphous and crystalline forms. These effects result in an increase in the surface area of metal systems that is stabilized by the formation of a thin oxide layer on the surface of the metal skeleton. Moreover, ultrasonic processes may cause phase segregation because of the crystallization of one of the components in metal alloys or in metal solutions.

Herein, we focus on the ultrasound-assisted modification of silicon. For applications related to optics<sup>[4a,b]</sup> or drug delivery,<sup>[4c,d]</sup> silicon suffers from an absence of intrinsic fluorescence and a lack of simple “green” modification techniques to render it suitable for such applications. In our study, we investigate the pronounced and controlled response of silicon surfaces to ultrasonic treatment, together with the formation of porous optically active silicon. This novel ultrasound-assisted method avoids the use of HF or similarly

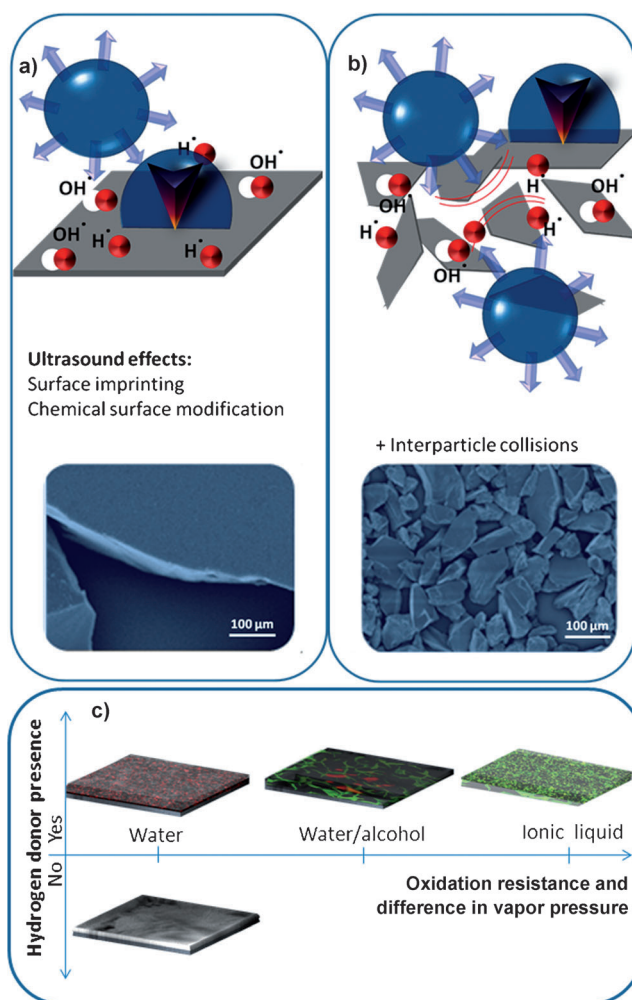


**Figure 1.** Ultrasonic effects (surface imprinting, interparticle collisions and chemical surface modification by free radicals) and initial SEM images of a) Si plates and b)  $\mu$ -sized Si particles. c) 3D schematic reconstruction, based on  $\mu$ -confocal and TEM measurements of photoluminescence and porosity change, respectively, of Si after sonication in controlled solvent conditions.

[\*] Dr. E. V. Skorb, Prof. H. Möhwald  
Interface Department, Max Planck Institute of Colloids and Interfaces  
Am Mühlenberg 1, 14476 Potsdam (Germany)  
E-mail: skorb@mpikg.mpg.de

Dr. D. V. Andreeva  
Physical Chemistry II, University of Bayreuth  
Universitätsstrasse 30, 95440 Bayreuth (Germany)

[\*\*] The authors gratefully acknowledge helpful discussions with Dr. Klaus Lips and Dr. Enno Malguth (Helmholtz-Zentrum Berlin für Materialien und Energie, Institut für Silizium-Photovoltaik). We thank Dr. Nelia Wanderka (Helmholtz-Zentrum Berlin für Materialien und Energie, Institut Angewandte Materialforschung) for kindly providing the HRTEM measurements. This work was generously supported by the Alexander von Humboldt Foundation, NATO CLG 984267 and SFB 840.

Supporting information for this article is available on the WWW under <http://dx.doi.org/10.1002/anie.201105084>.

aggressive media, which are detrimental to the environment.<sup>[4]</sup>

The ultrasound-assisted modification of silicon plates, in the form of both crystalline silicon wafers and amorphous silicon deposited onto glass, and  $\mu$ -sized particles is illustrated in Figure 1. In general, the interaction of cavitation bubbles with the silicon surface results in mechanical and chemical modification. The ultrasonic modification of solids is known to be controlled by various sonication conditions, including the intensity and duration of sonication, the solvent, and the

concentration and size of the sonicated species, oxidants, and reducing agents involved.<sup>[1,3,5]</sup>

The important innovation we introduce here is the addition of hydrogen donors during ultrasonication, which has dramatic influence on the process. The sonication of silicon species in water that does not contain a hydrogen donor results in the formation of an oxidized surface caused by the oxidation of the silicon by-products of water sonolysis. The samples are characterized by a slight increase in their surface roughness and the absence of photoluminescence (Figure 1c; see also the Supporting Information, Figure S1). The hydrogen donors slow the surface oxidation processes, which are brought on by free radicals formed during water sonolysis, and stabilize the porous structure through the formation of silicon-terminated bonds. In this case, Si–H bonds could be formed as an alternative to, or together with, Si–O bonds. The illustration in Figure 1c, based on a 3D reconstruction of TEM and  $\mu$ -confocal measurements of the surface after high-intensity ultrasonic exposure, shows our general concept of a single-step “green” method for the construction of surfaces with different porosities. Without a reducing agent present during modification in water, neither porous nor luminescent structures were observed. However, in the presence of a reducing agent, luminescent structures with a range of porosities (25–40% in water, 60–70% in water/alcohol mixtures, and 40–50% in an ionic liquid) were detected. Furthermore, the differences in porosities correlate with differences in photoluminescence (green or red).

We used Mg or Al in water and water/alcohol mixtures, or NaBH<sub>4</sub> in an ionic liquid as the hydrogen donors. The formation of hydrogen-terminated bonds on the surface of the silicon during ultrasonication could significantly slow or prevent surface oxidation, even in a water solution, as evidenced by infrared reflection absorption spectroscopy (IRRAS; Supporting Information, Figure S2). Figures 2a–d and S2 were obtained from wafer plate samples modified in the presence of hydrogen-donor species. The formation of channel-like structures was observed in samples prepared by 5 min of sonication. We have recently demonstrated similar modification features (channel-like structures) for metals.<sup>[3]</sup> Samples modified for 20 min reveal partial surface amorphization (Figure 2b), which later converts into a completely amorphous microporous silicon structure (Figure 2c). Thus, the hydrogen-donor materials stimulate the formation of Si–H bonds, which stabilize the ultrasonically formed structures and allow for the possible formation of nanocrystalline silicon (nc-Si). The formation of Si–H bonds is also indicated by the IRRA spectra (Supporting Information, Figure S2).

The structure of the modified silicon may influence the electronic properties, charge separation, optical properties, electroadsorption, and electroreflection. For certain applications,<sup>[4]</sup> the partially hydrogenated microporous silicon with visible red photoluminescence, as shown in Figure 2d, is advantageous. In water solutions, the photoluminescent centers are submicron sized and closely packed, which protects them from agglomeration; their cooperative effect is visible in  $\mu$ -confocal photoluminescence.

Numerous models<sup>[6]</sup> can be proposed to explain the photoluminescence of the modified silicon, including quan-

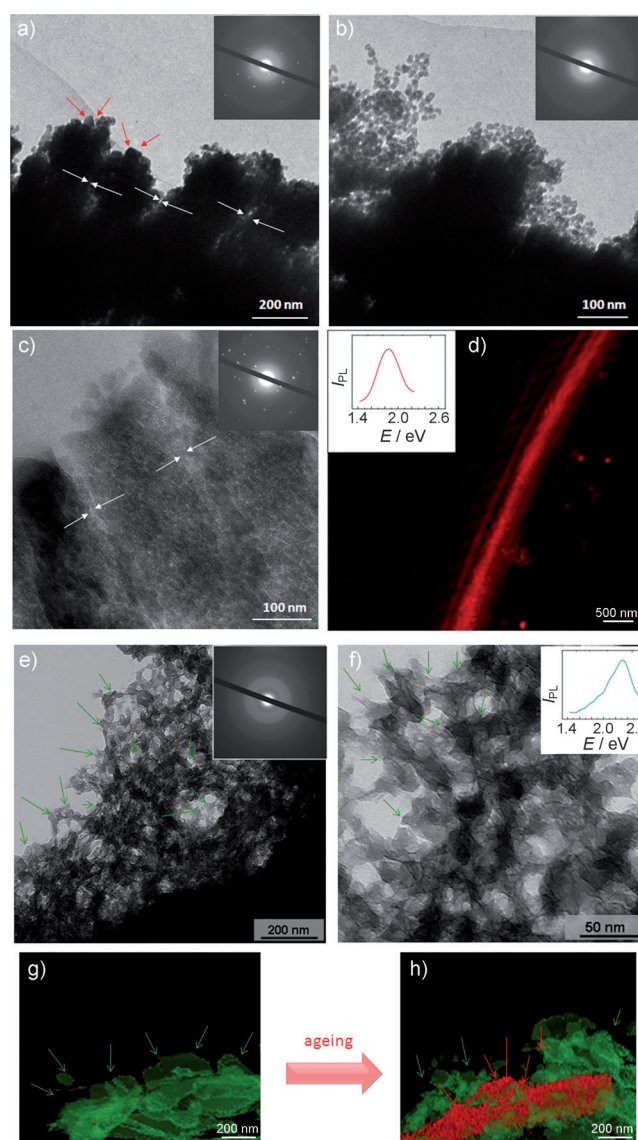


**Figure 2.** a–c) TEM images of the surface of ultrasonically modified silicon wafers in aqueous solution in the presence of a hydrogen-donor material (Mg powder) after a) 10 min, b) 20 min, and c) 30 min of modification. Insets (a–c) show electron-diffraction (ED) patterns of the samples modified for the corresponding time. d)  $\mu$ -confocal photoluminescence (PL) spectra (fluorescence mode, side view) of the silicon after 30 min of modification. Inset (d) shows the fluorescence emission spectrum of the surface. The preferable channel-like modification is shown by the white arrows. e, f) TEM images of the surface of a silicon wafer sonicated (20 kHz, 57 W cm<sup>−2</sup>) in a water/alcohol mixture (higher vapor pressure in comparison with water) in the presence of a hydrogen donor material (Mg powder) for 30 min. Insets show the corresponding ED (e) and fluorescence emission (f) spectra of the surface. g, h)  $\mu$ -Confocal PL spectra (fluorescent mode, side views) of silicon after 30 min of modification (g) followed by ageing (h). The green and red arrows show side views of the PL spectra.

tum confinement, surface states, defects in the oxide, and the formation of hydrogen-terminated bonds. Radiative recombination is another possibility, but of a different nature. Radiative recombination takes place within the surface amorphous layer. Surface states that localize electrons and



holes, either separately or together, subsequently recombine radiatively. A surface defect renders one undulation non-radiative, whereas an exciton localized in a neighboring undulation recombines radiatively. Radiative recombination occurs from the Si hydride bonds. Partially oxidized Si structures containing various defects can act as radiative centers in porous Si, for example, an oxygen shallow donor or a nonbridging oxygen hole center and a Si dangling bond. In this case, the luminescence of silicon sonicated in an aqueous solution can be explained by the formation of hydrogen-terminated bonds, and/or nonterminated bonds, and/or the formation of nc-Si in the porous matrix of SiO<sub>x</sub>.

Different solvents can stimulate various bubble-collapse scenarios.<sup>[7]</sup> The speed of the sonochemical processes and thus the production of excited species (radicals) strongly depends on the vapor pressure of the solvent. Therefore, surface oxidation by free radicals greatly depends on the nature of the solvent. In this study, we performed the sonication of silicon species in water, water-alcohol mixtures, and in ionic liquids (Figure 1). The modification of silicon in water/alcohol solutions (Figure 1) results in a decrease in the oxidizing ability; it also influences the kinetics owing to the higher vapor pressures of the solvent mixtures compared with that of water.<sup>[5b-d]</sup> Additionally, as shown in Figure 2 e–h, sonication in water/alcohol mixtures leads to silicon with a higher porosity than samples sonicated in water, with porosity ranging from the micro-scale to the meso-scale. Moreover, as shown in Figure 1 c and Figure 2 e–h, the character of the luminescence strongly depends on the conditions of sonication. The difference in photoluminescence, red after sonication in water and initially green after sonication in a water/alcohol mixture, involves the formation of a partially oxidized Si structure containing various defects, as well as hydrogen-terminated and/or nonterminated bonds.<sup>[6]</sup>

We can change the character of the photoluminescence from green to red, for example, in samples exposed to water, by aging and partially oxidizing the silicon (Figure 2 g, h), thus going through mostly hydrogen-terminated and/or nonterminated bonds to a partially oxidized Si structure. The light emitted by a single point on the silicon surface was estimated by a 3D reconstruction of the porous  $\mu$ -sized structure (Supporting Information, Figure S3). We conclude that the modification starts from the outer surface layers (Figure S3 a), as all of the fluorescent dots are located on the surface of sonochemically exposed samples. These dots are probably formed on the spots where bubble collapse occurs. Shock waves or liquid jets crashing into the surface introduce defects in the silicon and defect states. Further modification causes deeper modification of the silicon. Figure S3 b shows that the fluorescent centers are distributed both on the surface and in the matrix of porous silicon. Their emission changes from green to red because of the changes in the structures of the luminescent centers.<sup>[6]</sup>

It has been suggested that, in ionic liquids (IL), the oxidation could be avoided by simultaneous (re)crystallization, which could lead to green luminescence (Figure 1) vis-à-vis hydrogen-terminated and/or nonterminated bonds.<sup>[6]</sup> As shown in Figure 3 a, b, we are making progress towards process control, which is a high priority for this nonequili-

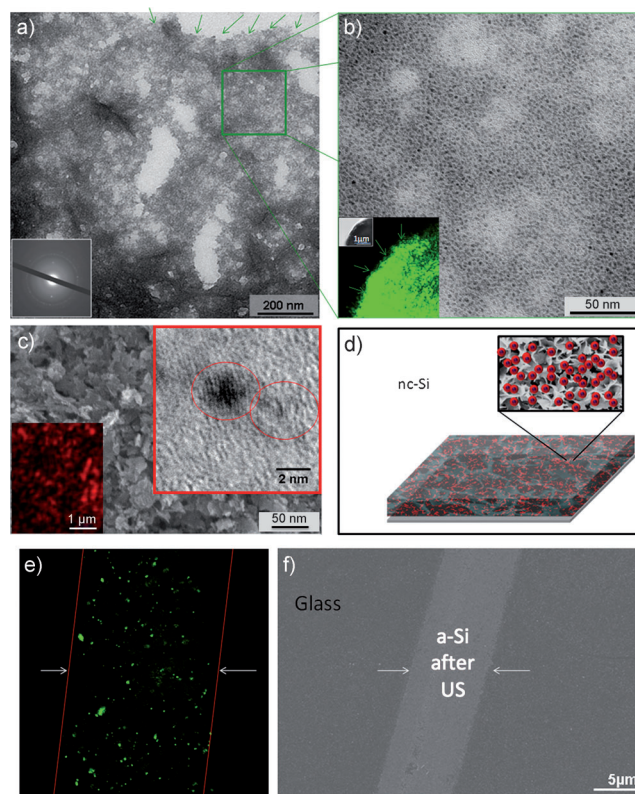


**Figure 3.** a, b) TEM images of the silicon surface after 30 min of sonication in 1-butyl-3-methylimidazolium chloride in the presence of a hydrogen donor material (NaBH<sub>4</sub>). Insets show corresponding electron-diffraction (a) and  $\mu$ -confocal photoluminescence (PL) (b) spectra (fluorescent and optical modes, side view). The green arrows show a side view of PL. c) SEM/HRTEM/ $\mu$ -confocal PL (fluorescent mode, top view) of the a-Si on the glass after sonication. d) Illustration of the formation of nc-Si in the porous matrix. e)  $\mu$ -confocal image in fluorescent mode of the a-Si patterned glass sonicated for 30 min in a water/alcohol mixture in the presence of a hydrogen donor material (Mg). The red lines and the white arrows show the pattern area. f) The corresponding SEM image.

brum process<sup>[1]</sup> using high-intensity ultrasound. In particular, applying the method in solvents with a negligible vapor pressure,<sup>[7]</sup> such as the ionic liquid 1-butyl-3-methylimidazolium chloride, allows the formation of structures with medium (40–50 %) porosity, although with an irregular pore distribution (Figure 3 a, b). Moreover, the formation of nc-Si in the silicon matrix is clearly visible (Figure 3 b).

We also confirmed that pronounced modification of amorphous silicon (a-Si), such as silicon deposited onto glass, which is used in advanced techniques for photovoltaic devices,<sup>[8]</sup> is possible. Figure 3 c, d shows that a pronounced surface roughness can be achieved with simultaneous local crystallization and red-photoluminescent nc-Si formation, as well as formation of partially oxidized Si structures containing various defects.

Because the degree of structural order in solid silicon can be locally changed while simultaneously achieving photoluminescence, the development of a technique for the modification of patterned surfaces (Figure 3 e, f) with the

formation of distributed luminescent spots is possible. Patterns can be produced by ion-beam-assisted vacuum deposition, which has been used to deposit amorphous silicon onto glass through a specific mask that protects some areas from deposition, thus allowing for surface patterning.<sup>[8]</sup>

We performed an additional experiment on particles of silicon (ca. 100  $\mu\text{m}$  diameter) to prove that the formation and subsequent phase transitions (crystalline–amorphous–crystalline) of nc-Si are possible without oxidation in water solution in the presence of a hydrogen donor. The  $\mu$ -sized particles were modified within 35 min of sonication (Figure 4).

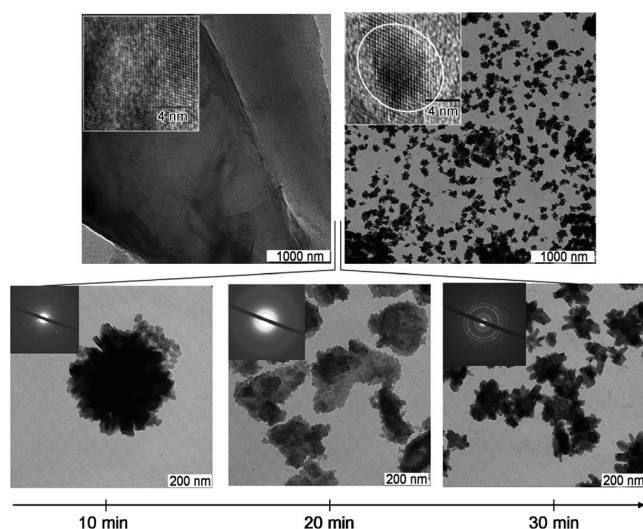


**Figure 4.** TEM images of  $\mu$ -sized silicon particles modified by ultrasonication in aqueous solution in the presence of a hydrogen-donor material (Mg) before and after a 35 min modification (upper left and right images, respectively). The HRTEM images (upper insets) show the crystalline structure. The bottom images are the TEM/electron-diffraction images vs. modification time (10 min (left), 20 min (middle) and 30 min (right)). The observed modification kinetics are faster than those observed with plates.

The resulting particles exhibit a pronounced crystalline structure, and their size decreases to the submicron scale. The amorphization of the particles is observed within 20 min of modification. Further exposure ( $> 30$  min) causes well-pronounced crystal growth from the amorphous phase, as well as a further size decrease (Figure 4; see also the Supporting Information, Figure S4). The observed phase transition (between crystalline and amorphous) is probably the main factor responsible for ultrasound-assisted silicon modification. The special conditions provided by high-intensity ultrasound could affect the melting and growth of the silicon crystals. The form of a solidified microstructure can be controlled by fast local heating and cooling cycles provided by cavitation. The crystal formation depends upon the difference between the rates of attachment and detachment of atoms at the interface. The rate of attachment depends on the rate of diffusion in the liquid and therefore is affected by sonication.

We have demonstrated the formation of porous silicon with unique optical properties through a “green” method of ultrasonication including: 1) the one-step formation of silicon

with a purposefully variable porous structure, 2) the formation of photoluminescent centers and defect states that could be centers for charge separation, and 3) the possibility of patterned surface-selective modification. The high potential of ultrasound results from the interplay of different mechanisms (Figure 1), and the silicon modification demonstrated here relies on this interplay. Nucleation and bubble collapse affect the surface of a material. First, fast silicon oxidation could be avoided by the possible formation of structure-stabilizing bonds; in this case, by hydrogenation. Next, the solid is modified further, with pores formed deep inside. This process requires material transport over  $\mu\text{m}$  dimensions during the bubble collapse and following the stabilization of the material. Moreover, the kinetics of the process are highly dependent on the solvent. Thus, solvents with higher vapor pressures than water allow the porosity to be tuned while also allowing the manipulation of the oxidizing ability of the solvent. These modifications influence the nature of the luminescent centers, suggest possible silicon pathways in IL, and allow us to propose mechanisms for the modification of materials with different initial crystallinities, as well as with patterned surfaces. The findings presented here provide guidelines for the expansion of the concept towards a broad variety of systems. Thus, the possibility of ultrasonic structure formation enables the use of a “green” medium under ambient conditions in previously inaccessible areas of material science.

## Experimental Section

Silicon wafers (Sigma–Aldrich), 2-propanol (Alfa Aesar), 1-butyl-3-methylimidazolium chloride (Sigma–Aldrich), magnesium powder (325 mesh, 99.8%, Alfa Aesar), and sodium borohydride (Sigma–Aldrich) were used as received. Water was purified prior to use in a three-stage Millipore Milli-Q Plus 185 purification system, and exhibited a resistivity greater than  $18.2 \text{ M}\Omega \text{ cm}^{-1}$ . Silicon wafers were degreased in flowing 2-propanol and rinsed in purified water. The  $\mu$ -Si particles were obtained through the milling of wafers.

Ultrasonic treatment was carried out in a thermostated reactor (65 °C). The unit VIP1000hd (Hielscher, Germany) was operated at 20 kHz, with a maximal electric output of 1000 W, and equipped with an ultrasonic horn BS2d22 (head area of  $3.8 \text{ cm}^2$ ) and a booster (B2-1.2).

Scanning electron microscopy (SEM) measurements were conducted with a Gemini Leo 1550 instrument at an operating voltage of 3 keV. Transmission electron microscopy (TEM) measurements were performed on a Zeiss EM 912 Omega (Carl Zeiss AG, Germany) transmission electron microscope operated at 300 kV and equipped with an electron-diffraction (ED) unit. The unit cell and symmetry of an unknown phase that has been determined from the geometry of the diffraction pattern with the proper interpretation of the intensities of spots yields the positions of atoms in the crystal. High-resolution transmission electron microscopy (HRTEM) was performed by TEM in a Philips CM30 operated at 300 kV. The samples were ultramicrotomed (Leica EM FC6) and placed onto carbon-coated copper grids.

The photoluminescence (PL) spectra were obtained at room temperature using either a pulsed-excitation nitrogen laser (337 nm) or a continuous-excitation HeCd laser (325 nm). The luminescence spectra were measured using a Jobin–Yvon H20 monochromator and a Hamamatsu TV R316 or R712 photomultiplier cooled to  $-20^\circ\text{C}$ . The  $\mu$ -confocal PL was measured by confocal laser scanning microscopy (CLSM, Leica, Germany), which is an important

method for obtaining high-fluorescence (red-green) and transmission-mode resolution images and for 3D reconstructions.

Received: July 20, 2011

Revised: December 2, 2011

Published online: April 5, 2012

**Keywords:** luminescence · porous materials · silicon · sonochemistry · ultrasound

- [1] a) *Chemistry with ultrasound. Critical reports on applied chemistry* (Ed.: T. J. Mason), Elsevier, Essex, **1990**; b) *Ultrasound, It's Chemical, Physical, and Biological Effects* (Ed.: K. S. Suslick), Wiley-VCH, Weinheim, **1989**; c) G. Cravotto, P. Cintas, *Angew. Chem.* **2007**, *119*, 5573–5575; *Angew. Chem. Int. Ed.* **2007**, *46*, 5476–5478; d) *Sonochemistry and Cavitation* (Ed.: M. A. Margulis), Gordon & Breach, London, **1995**; e) K. S. Suslick, G. J. Price, *Annu. Rev. Mater. Sci.* **1999**, *29*, 295–326.
- [2] a) *Sonochemistry and sonoluminescence. Series C: Mathematical and Physical Science* (Eds.: L. A. Crum, T. J. Mason, J. L. Reisse, K. S. Suslick), NATO ASI Series, Kluwer Academic Publishers, Dordrecht, **1999**; b) N. A. Tsochatzidis, P. Guiraud, A. M. Wilhelm, H. Delmas, *Chem. Eng. Sci.* **2001**, *56*, 1831–1840.
- [3] a) E. V. Skorb, D. Fix, D. G. Shchukin, H. Möhwald, D. V. Sviridov, R. Mousa, N. Wanderka, J. Schäferhans, N. Pazos-Pérez, A. Fery, D. V. Andreeva, *Nanoscale* **2011**, *3*, 985–993; b) E. V. Skorb, H. Möhwald, T. Irrgang, A. Fery, D. V. Andreeva, *Chem. Commun.* **2010**, *46*, 7897–7899; c) J. Gensel, T. Borke, N. Pazos Pérez, A. Fery, D. V. Andreeva, E. Betthausen, A. H. E. Müller, H. Möhwald, E. V. Skorb, *Adv. Mater.* **2012**, *24*, 985–989; d) D. V. Andreeva, D. V. Sviridov, A. Masic, H. Möhwald, E. V. Skorb, *Small* **2012**, *8*, 820–825.
- [4] a) L. T. Canham, *Nature* **2000**, *408*, 411–412; b) J. D. Holmes, K. P. Johnston, R. C. Doty, B. A. Korgel, *Science* **2000**, *287*, 1471–1473; c) Y. Y. Li, F. Cunin, J. R. Link, T. Gao, R. E. Betts, S. H. Reiver, V. Chin, S. N. Bhatia, M. J. Sailor, *Science* **2003**, *299*, 2045–2047; d) C. Gurtner, A. W. Wun, M. J. Sailor, *Angew. Chem.* **1999**, *111*, 2132–2135; *Angew. Chem. Int. Ed.* **1999**, *38*, 1966–1968.
- [5] a) E. V. Skorb, D. G. Shchukin, H. Möhwald, D. V. Andreeva, *Nanoscale* **2010**, *2*, 722–727; b) K. S. Suslick, J. J. Gawienowski, P. F. Schubert, H. H. Wang, *Ultrasonics* **1984**, *33*–36; c) B. A. Oakley, G. Barber, T. Worden, D. Hanna, *J. Phys. Chem. Ref. Data* **2003**, *32*, 1501–1533; d) L. H. Thompson, L. K. Doraiswamy, *Ind. Eng. Chem. Res.* **1999**, *38*, 1215–1249; e) D. G. Shchukin, E. V. Skorb, V. Belova, H. Möhwald, *Adv. Mater.* **2011**, *23*, 1922–1934.
- [6] a) L. Pavesi, L. D. Negro, C. Mazzoleni, G. Franzo, F. Priolo, *Nature* **2000**, *408*, 440–444; b) A. G. Cullisa, L. T. Canham, P. D. J. Calcott, *J. Appl. Phys.* **1997**, *82*, 909–965; c) M. V. Wolkin, J. Jorne, P. M. Fauchet, *Phys. Rev. Lett.* **1999**, *82*, 197–200.
- [7] a) P. M. Kanthale, M. Ashokkumar, F. Grieser, *Phys. Chem. Lett. C* **2007**, *111*, 18461–18463; b) D. S. Jacob, V. Kahlenberg, K. Wurst, L. A. Solovyov, I. Felner, L. Shimon, H. E. Gottlieb, A. Gedanken, *Eur. J. Inorg. Chem.* **2005**, 522–528.
- [8] C. Boehme, K. Lips in *Charge Transport in Disordered Solids with Applications in Electronics, Vol. 5* (Ed.: S. Baranovski), Wiley, Chichester, **2006**, pp. 179–219.